

Friction and wear properties of ZrO₂/SiO₂ composite nanoparticles

Wei Li · Shaohua Zheng · Bingqiang Cao · Shiyu Ma

Received: 3 March 2010 / Accepted: 22 May 2010 / Published online: 15 June 2010
© Springer Science+Business Media B.V. 2010

Abstract In this article, the lubrication properties of ZrO₂/SiO₂ composite nanoparticles modified with aluminum zirconium coupling agent as additives in lubricating oil under variable applied load and concentration fraction were reported. It was demonstrated that the modified nanoparticles as additives in lubrication can effectively improve the lubricating properties. Under an optimized concentration of 0.1 wt%, the average friction coefficient was reduced by 16.24%. This was because the nanoparticles go into the friction zone with the flow of lubricant, and then the sliding friction changed to rolling friction with a result of the reduction of the friction coefficient.

Keywords ZrO₂/SiO₂ · Additive · Friction · Self-repairing · Lubrication · Colloids

Introduction

As the viscosity of a lubricant decreases, the frictional force in the hydrodynamic lubrication regime decreases. The decrease of the lubricant viscosity causes a lower extreme pressure of the lubricant, so the friction surface is damaged at high load due to the metal contact, which makes reliability worse (Lee

et al. 2009). With the development of nanostructured materials in the recent years, attempts were made to use nanoparticles as lubricant additives to improve their lubrication properties (Song and Zhang 2008). When some nanoparticles were added into the lubricating oil, their lubrication properties can be effectively improved (Red'kin 2004; Hu and Dong 1998; Dong et al. 1998; Guo et al. 2009), which is better than the traditional solid lubricant additives and becomes a promising new lubricating material. A previous study revealed that nano-lubricant which was a mixture of nanoparticles and lubricating oil increased the extreme pressure of the lubricant and reduced the friction coefficient, which could make the bearing more durable (Kwangho et al. 2009; Murakami et al. 2007). Zhang et al. (2009) reported that using CaCO₃ nanoparticles as PAO base oil additives can dramatically improve the load-carrying capacity, as well as the anti-wear and friction reduction properties of PAO base oil. In addition, higher applied load, moderate frequency, longer duration time, and lower temperatures were beneficial to the deposition of CaCO₃ nanoparticles accumulating on rubbing surfaces. Jee and Lee (2009) showed that the surface-functionalized diamond nanoparticles were highly dispersive and stable in oil, and can be used as lubricating oil additives without further modifications.

It has been reported that the main mechanism of the friction reduction when nanoparticles were added can be attributed to rolling/sliding effect (Wu et al. 2007; Chin-as-Castillo and Spikes 2003), protective

W. Li · S. Zheng (✉) · B. Cao · S. Ma
School of Materials Science and Engineering,
University of Jinan, Jinan 250022, China
e-mail: mse_zhengsh@ujn.edu.cn

film (Hu et al. 2002; Zhou et al. 2007), third-body effect (Rapoport et al. 2003), and mending effect (Liu et al. 2004). It is also found that there are different interactions when two or more nanoparticles lubricant additives are added, such as adduct effect, synergy, and antagonism effects (Sui et al. 2009). Although these effects have obvious influence on the performance of lubricating oil when nanoparticles were used as additives, the present study is few and highly needed.

In this article, $\text{ZrO}_2/\text{SiO}_2$ composite nanoparticles were prepared with in situ modified method and surface was modified by aluminum zirconium coupling agent. Such modified $\text{ZrO}_2/\text{SiO}_2$ nanoparticles showed good dispersion stability in the lubricant. In order to estimate the ranges of application of $\text{ZrO}_2/\text{SiO}_2$ composite nanoparticles used as lubricating oil additive, the friction test was designed by four balls tester. The lubricative properties of $\text{ZrO}_2/\text{SiO}_2$ composite nanoparticles as additives in lubricating oil under variable load and concentration fraction were evaluated. In addition, the possible lubrication and anti-wear mechanism was discussed.

Experimental

The superficial modification of $\text{ZrO}_2/\text{SiO}_2$ composite nanoparticles

Zirconium acetate was added to 100 mL alcohol (95%) and heated stirring to form a sol. The pH value was set at 9–10 by ammonia dropping. After three times washing with alcohol (95%), ZrO_2 precursor was prepared; 0.025 mol TEOS was added to 100 mL alcohol (95%), then the ZrO_2 precursor was added. Next 0.026 g ammonium hydrogen fluoride was added and heated stirring to form a sol. The pH value was set at 9–10 by ammonia dropping. After three times washing with alcohol (95%), $\text{ZrO}_2/\text{SiO}_2$ precursor was prepared; the $\text{ZrO}_2/\text{SiO}_2$ precursor was dissolved with 150 mL alcohol (95%). The aluminum zirconium coupling agent was added and the concentration was 0.6 wt%. The solution was mixed 1.5 h before put into the autoclave. The reaction conditions were set as follows: temperature 220 °C, pressure 3.6 MPa, time 2 h. The powder was put out until the reactor cooled to room temperature. Then the modified $\text{ZrO}_2/\text{SiO}_2$ composite nanoparticles

were made. Such modified ZrO_2 particles and SiO_2 particles were homogenously mixed together. The interaction between the nanoparticles achieved the best. The composite nanoparticles particle size, morphology, and modification effect were observed with transmission electron microscopy (TEM) and Zeta potential analyzer. The absorbency of nano-oil was measured with an ultraviolet spectrophotometer.

Anti-wear friction test

The anti-wear friction properties were tested by a four balls tester (MMU-10G, Jinan). The modified $\text{ZrO}_2/\text{SiO}_2$ composite nanoparticles were added into lubricating oil (#20) under different concentration fraction (mass concentrations were: 0, 0.05, 0.1, 0.3, 0.5, 0.75, and 1 wt%). For each concentration, the fraction coefficients were measured five times and then averaged to ensure the data accuracy. The oil solution was dispersed with ultrasonic for 30 min and then nano-oil was obtained. The operation process was shown in Fig. 1. Then the nanoparticles were homogenously dispersed in the lubricating oil. The nano-oil was kept at room temperature for 48 h. Then wear friction and wear tests were performed with a four balls tester. The experimental data was recorded in situ and the test data were acquired with a computer automatically.

Four-ball friction and wear test

In four-ball friction process, the three balls located below were tightly fixed, as shown in Fig. 2. The top

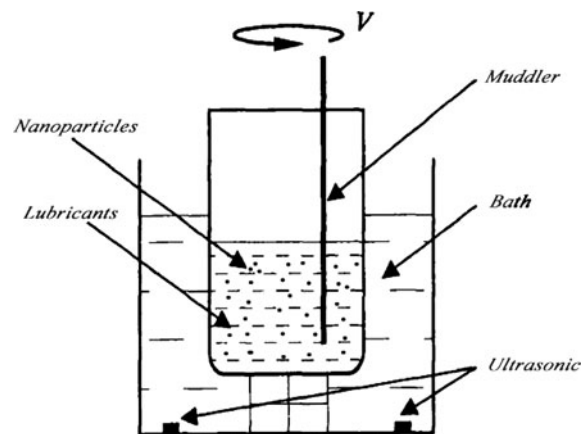


Fig. 1 Preparation setup and process of the nano-oil measured in this article

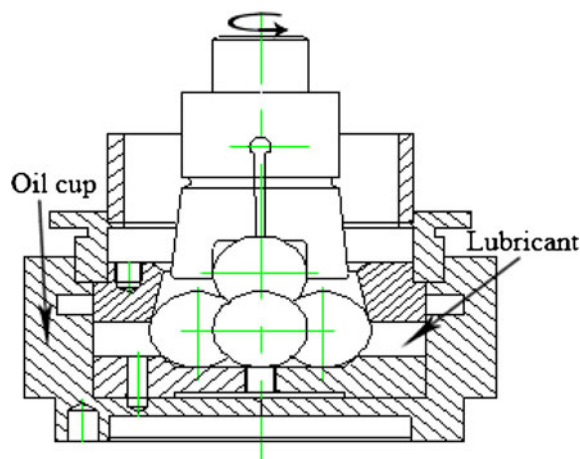


Fig. 2 The structural sketch map of four-ball friction and wear test

ball was driven and rotated on the three supporting balls. Four-ball wear test parameters were set as follows: temperature at 75 °C, speed of 1,450 r/min, load at 147 N, and time of 30 min. The ball was in accordance with the steel ball GB/308-89 manufacturing, GCr15, two steel balls, diameter 12.7 mm; hardness 64–66HRC. Friction coefficient was recorded by the data terminal processing systems. The size of wear scar diameter was observed with a metallographic microscope and then the average size of wear scar diameter was obtained.

Thrust ring friction and wear test

In thrust ring friction process, the test loop was suspended in order to push the ring in the form of surface contact friction, as shown in Fig. 3. The friction coefficient, wear volume and changes in surface morphology of friction pairs were obtained. After each experiment, the surface of friction pair was washed with petroleum ether, so that there were no impurities on the surface and the quality changes were accurately measured. Friction coefficient was recorded by the data terminal processing systems. The wear quality changes were recorded by the electronic balance. The friction pair surface morphology was observed with SEM. Thrust ring wear test parameters were set as follows: temperature at 75 °C, speed of 1,200 r/min, load at 200 N, and time of 30 min. The thrust ring is 45 # steel, hardened to 45–50HRC, outside diameter of 50 mm, inner

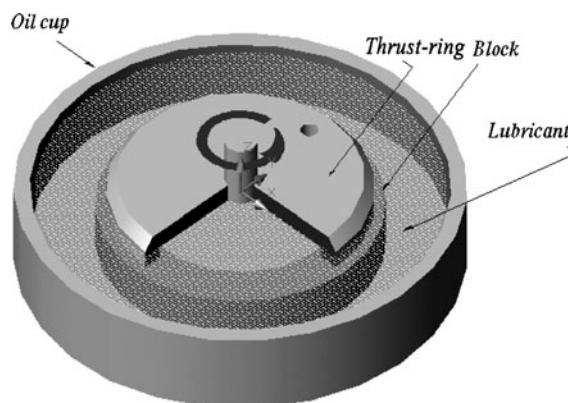


Fig. 3 The structural sketch map of thrust ring friction and wear test

diameter of 42 mm, and thickness of 5 mm; test ring is 45 # steel, hardened to 44–46HRC, outside diameter of 54 mm, inner diameter of 38 mm, and thickness of 10 mm.

Results and discussion

Effect of surface modification

Dispersibility stability analysis

The agglomerating between nanoparticles was characterized with the Zeta potential value. The bigger absolute value means the nanoparticles disperse more homogeneously. The absolute value of $\text{ZrO}_2/\text{SiO}_2$ Zeta potential was shown in Fig. 4. As shown in Fig. 4, Zeta potential absolute value of modified $\text{ZrO}_2/\text{SiO}_2$ nanoparticles was greater than that of as-prepared $\text{ZrO}_2/\text{SiO}_2$ nanoparticles. This indicated that static repellency of modified $\text{ZrO}_2/\text{SiO}_2$ became stronger than the as-prepared nanoparticles. The modified $\text{ZrO}_2/\text{SiO}_2$ was well dispersed in lubricating oil.

Figure 5 is the TEM image of the $\text{ZrO}_2/\text{SiO}_2$ composite nanoparticles. As shown in Fig. 5a, some $\text{ZrO}_2/\text{SiO}_2$ nanoparticles agglomerated. However, the modified nanoparticles were well dispersed and their sizes were rather uniform of 50–80 nm. The distribution of large particles was less, almost no agglomeration, as shown in Fig. 5b. It was demonstrated that the specific surface area of the modified $\text{ZrO}_2/\text{SiO}_2$ composite nanoparticles was reduced significantly, and the surface activity was also decreased. Finally,

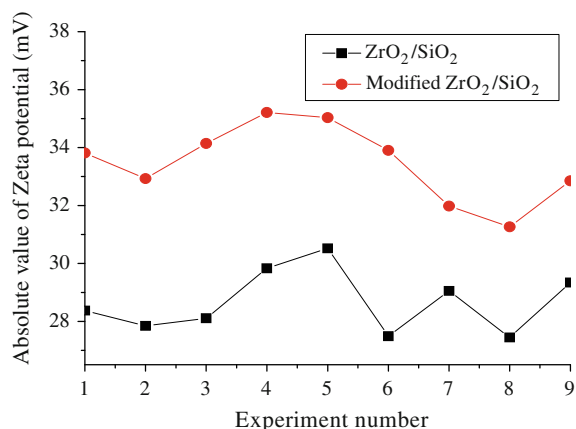


Fig. 4 The absolute value of ZrO₂/SiO₂ nanoparticles Zeta potential

the aggregation of the nanoparticles was effectively inhibited. The dispersion stability of nanoparticles was greatly enhanced.

Oil-soluble analysis

The ZrO₂/SiO₂ nanoparticles were added into lubricating oil and then the absorbency of nano-oil with time was observed by ultraviolet spectrophotometer, as shown in Fig. 6. The absorbency should be greater if the dispersion of nano-oil is better. After 56 h, the absorbency of nano-oil with modified ZrO₂/SiO₂ nanoparticles was still stable. However, the nano-oil with as-prepared ZrO₂/SiO₂ nanoparticles showed some precipitates. The absorbency showed decreasing of 3.5% in 76 h for functionalized particles, but 7% for as-prepared particles. The modified ZrO₂/SiO₂ nanoparticles can steadily disperse in lubricating oil. The images shown in Fig. 7 were taken after the oil was kept at room temperature for 12 h. As can be seen from Fig. 7a, the as-prepared ZrO₂/SiO₂ nanoparticles precipitated at the bottom of the bottle. However, the modified ZrO₂/SiO₂ nanoparticles were well dispersed in the oil (Fig. 7b). This is because that the surface of nanoparticles changed from inorganic phase to organic phase. This was due to that aluminum zirconium coupling agents bond with the ZrO₂/SiO₂ composite nano-particle surface hydroxyl. The role mechanism was shown in Fig. 8. The surface of ZrO₂/SiO₂ composite nanoparticles was successfully modified.

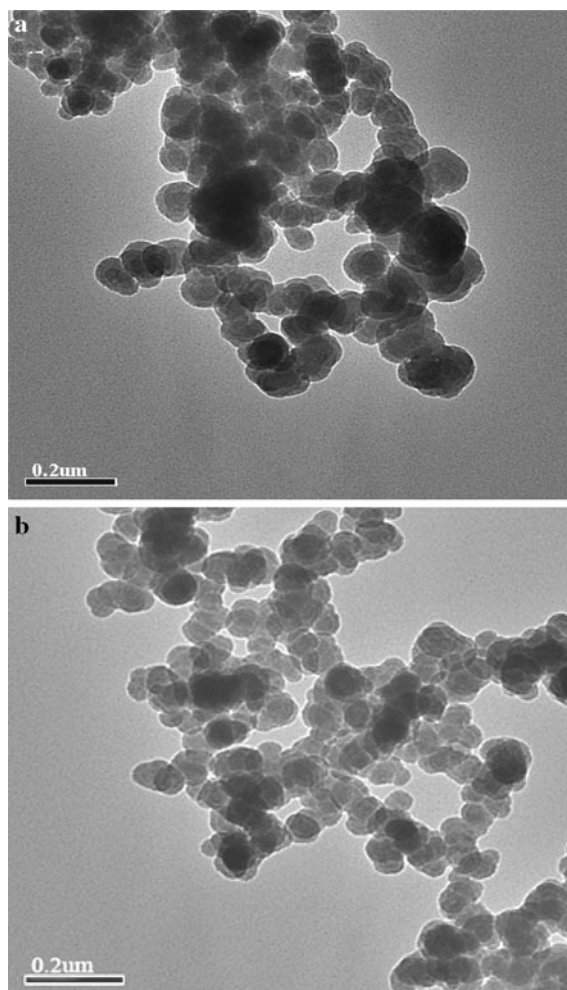


Fig. 5 The TEM image of ZrO₂/SiO₂ composite nanoparticles. **a** As-prepared ZrO₂/SiO₂ nanoparticles and **b** modified ZrO₂/SiO₂ nanoparticles

Friction and wear test

Four-ball test friction coefficient analysis

Figure 9 showed friction coefficient changes with the concentration fraction of ZrO₂/SiO₂ composite nanoparticles in lubricant oil. The friction coefficient decreased with the ZrO₂/SiO₂ concentration increased when the concentration was <0.1 wt%. However, the coefficient began to increase when the additive concentration was >0.1 wt%, as shown in Fig. 9. The reason was that, due to the flash temperature caused by the friction, the nanoparticles

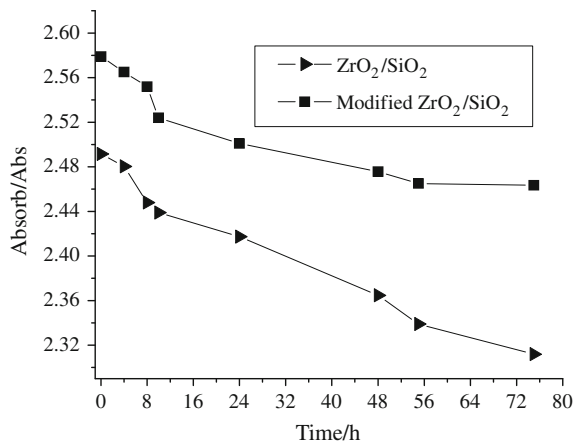


Fig. 6 The absorbency curve of nano-oil with time

adsorbed chemically on the metal friction surface through hydroxyl (Hu et al. 1998; Sun et al. 2002; Merschdorf 2002). At the same time, nanoparticles go into the friction zone with the flow of lubricant. Then the sliding friction was changed into rolling friction between the friction pair (Xu et al. 1997) with the result of the reducing friction coefficient. The lubrication mechanism was shown in Fig. 11. When fewer nanoparticles were added, e.g., 0.05 wt%, the friction zone cannot be completely filled. Therefore, the ball bearing effect cannot play and anti-friction effect was not obvious. When more nanoparticles were added, e.g., 0.5 or 1 wt%, nanoparticles were sintered into blocks by friction. Therefore, larger nanoparticles as impurities scratched the friction surface and the friction coefficient increased. Therefore, only when the added amounts of nanoparticles were in an optimal concentration range, the friction-reducing effect is better. As shown in Fig. 10, the friction-reducing effect was more effective at the additives concentration of 0.1 wt% with an average friction coefficient decreasing of 16.24%.

Four-ball test wear scar diameter analysis

Table 1 showed the diameter of wear scar on the balls in the lubricant oil with different concentration of nanoparticles. When the concentration was 0.1 wt%, the average size of wear scar diameter was the smallest. Figure 12 compares the wear scar morphologies of ball in lubricant oil with and without of the ZrO₂/SiO₂ nanoparticles. When no nanoparticles

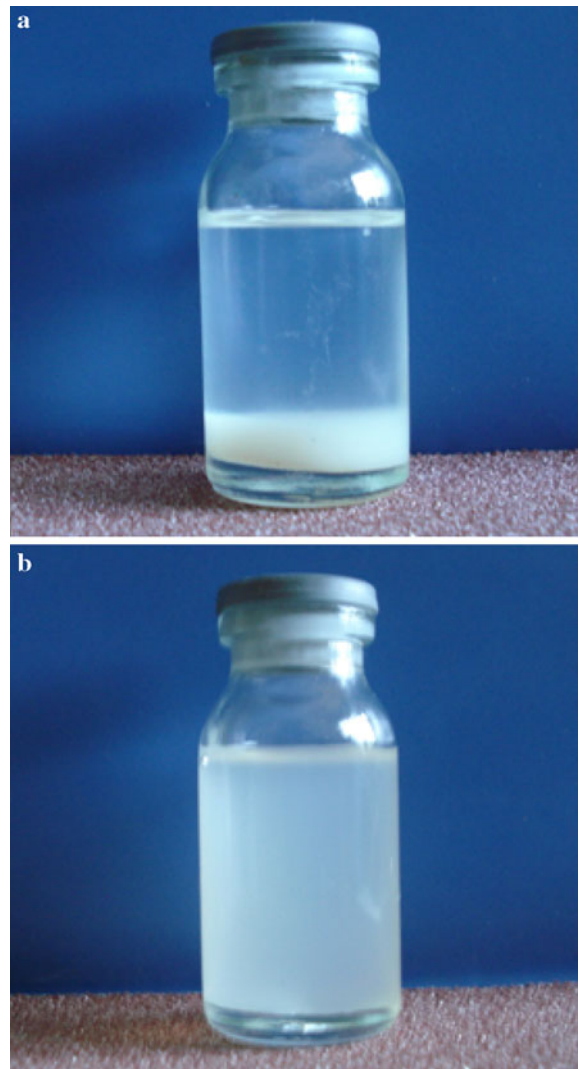


Fig. 7 The images of oil solution with different nanoparticles after 12 h. **a** With as-prepared ZrO₂/SiO₂ nanoparticles and **b** with modified ZrO₂/SiO₂ nanoparticles

were added, the vertical wear scar diameter of ball was 422.37 μm , as shown in Fig. 12a. Also the wear scar was deep and furrow from the existence of wear and tear rather than the elastic deformation. However, when the additives concentration was 0.1 wt%, the longitudinal wear scar diameter was 360.73 μm , as shown in Fig. 12b. While wear scar diameter was reduced by 61.64 μm , reduced the rate of 14.59%. These showed that the lubricating oil by adding a certain amount of modification ZrO₂/SiO₂ composite nanoparticles could play well anti-wear effects in the friction pairs (Kato and Komai 2007).

Fig. 8 The role mechanism of aluminum zirconium coupling agent

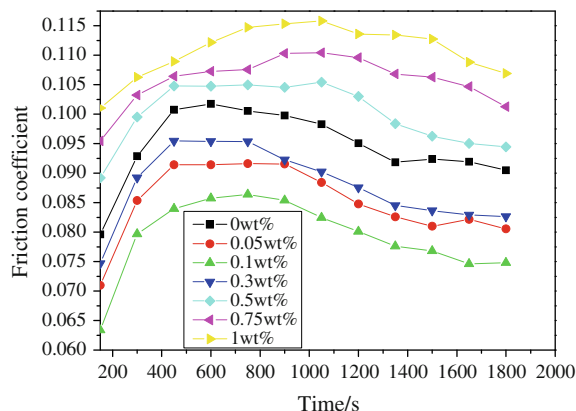
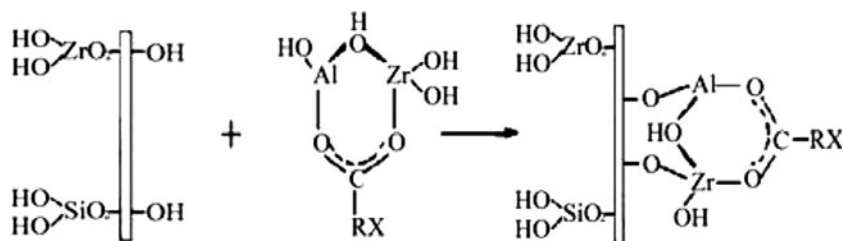


Fig. 9 Variation of friction coefficients with times in four-ball test

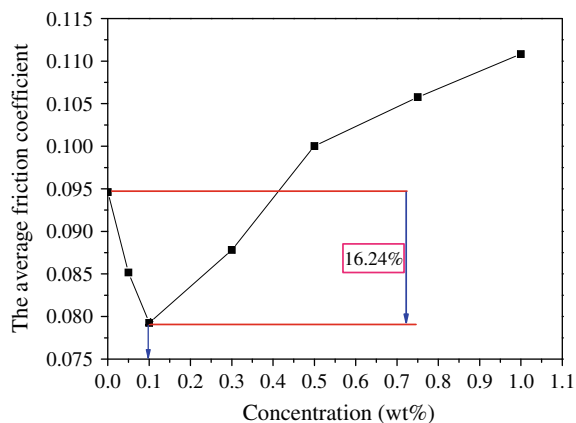


Fig. 10 Variation of the average friction coefficients with concentration fraction

Thrust ring wear test quality analysis

Table 2 showed the average mass loss of the thrust ring after the wear test when $\text{ZrO}_2/\text{SiO}_2$ additives of different concentration were used. The weight loss decreased with the $\text{ZrO}_2/\text{SiO}_2$ concentration increases when the concentration was <0.1 wt%. However, the

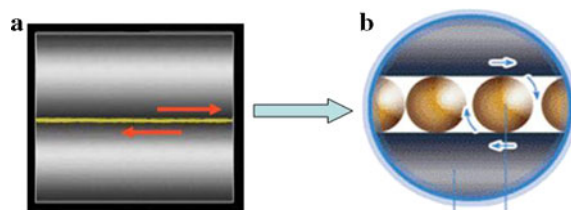


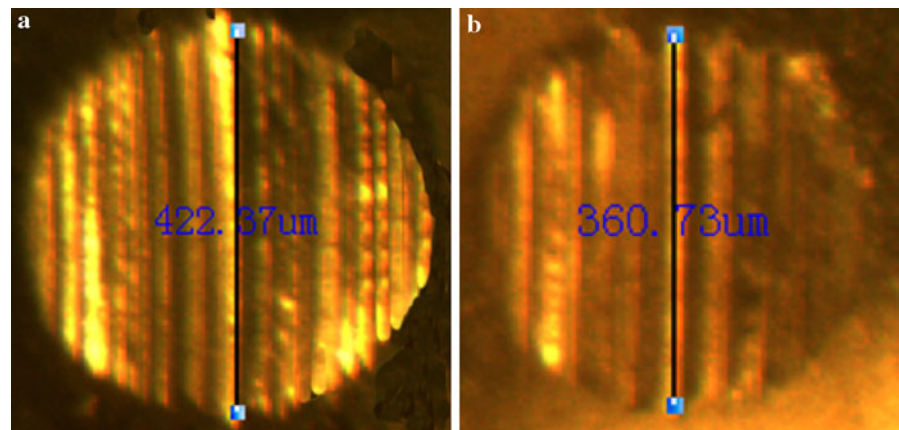
Fig. 11 The micro image of lubrication mechanism. **a** Sliding friction and **b** rolling friction

Table 1 The diameter of wear scar of the balls dispersed in the oil with different concentration of nanoparticles

	1	2	3	4	5	Average (μm)
0 wt%	422.37	421.68	421.35	422.96	423.49	422.37
0.05 wt%	380.89	381.02	380.96	379.26	379.17	380.26
0.1 wt%	360.40	361.35	360.73	359.64	361.53	360.73
0.3 wt%	386.97	385.99	386.51	385.24	386.99	386.34
0.5 wt%	430.93	429.24	429.83	431.03	429.82	430.17
0.75 wt%	432.26	433.89	434.02	433.54	431.74	433.29
1 wt%	439.12	438.96	440.12	439.79	441.06	439.81

weight loss began to increase when the additive concentration was >0.1 wt%, which was consistent with Figs. 9 and 10. In addition, when the nanoparticles adding amount was 0.1 wt%, the negative wear and tear was obtained. It can be explained with the dynamic self-healing deposition mechanism (Song and Zhang 2006). That was, mass loss caused by friction and nanoparticles deposition onto the friction pair surface coexisted. When the wear and tear was faster than the deposition, the mass lost happened. Otherwise, the thrust ring mass increased. When the concentration of $\text{ZrO}_2/\text{SiO}_2$ composite nanoparticles was 0.1 wt%, the performance of negative wear and tear was observed, which was caused by the dynamic self-healing mechanism of deposition, as shown in Fig. 13.

Fig. 12 Wear scar morphology of four-ball test (60 \times). **a** Lubricated by #20 mechanical oil with 0 wt% $\text{ZrO}_2/\text{SiO}_2$ and **b** lubricated by #20 mechanical oil with 0.1 wt% $\text{ZrO}_2/\text{SiO}_2$



Thrust ring test friction surface analysis

Figure 14 shows the SEM image of the thrust ring friction surface. As can be seen from Fig. 14a, when the lubricating oil without additives was used in the friction tests, noticeable scratches and furrows were clearly observed on the thrust ring surface. However, when $\text{ZrO}_2/\text{SiO}_2$ composite nanoparticles of 0.1 wt% were added into the same lubricating oil, the furrows were much shallower and narrower, as shown in Fig. 14b. At the same time, some white nanoparticle sediments were observed on the surface, which were filled into the scratches as indicated in the white box of Fig. 14b. It meant that some composite nanoparticles deposited onto the friction surface during the friction process.

Due to the small nanoparticle size, they can easily move into the worn area under the compressive stress of lubricating oil. Then a self-laminating film was formed on the friction surface, which can repair the surface (Huang et al. 2006). Moreover, low-energy electrons were released into lubrication medium during the friction process, and the positive and negative electric charge was produced in the friction pair's surface. Then, the released electrons combined with the chemical additives and anions or free radicals were formed, $\text{M} + \text{e} \rightarrow (\text{MR}) + {}^+\text{R}$. Finally, free radical R covered the friction pair's surface with

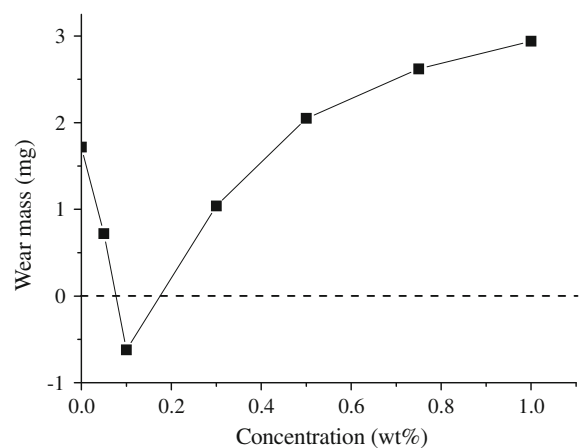


Fig. 13 Variation of the average wear mass with concentration fraction

silicon dioxide or zirconium. Therefore, the nanometer granule became protective film in the friction pairs face shape under this physical chemistry dual function (Merschdorf 2002). The forming mechanism was schematically shown in Fig. 15. This layer existed in solid state after the friction, and repaired dent friction surface. As can be seen from Fig. 14b, surface scratch of thrust ring changed smooth. The plow furrow was shallow, and the surface had the white deposit to appear.

Table 2 The average weight mass of the thrust ring

Concentration	0 wt%	0.05 wt%	0.1 wt%	0.3 wt%	0.5 wt%	0.75 wt%	1 wt%
Wear mass (mg)	1.72	0.72	-0.62	1.04	2.05	2.62	2.94

Fig. 14 The morphology of the wear scar on ring-on-block test. **a** Ring (0 wt%) and **b** ring (0.1 wt%)

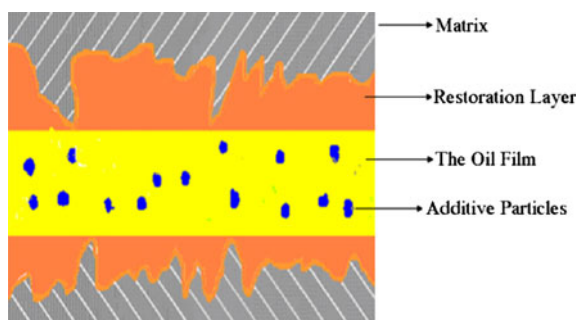
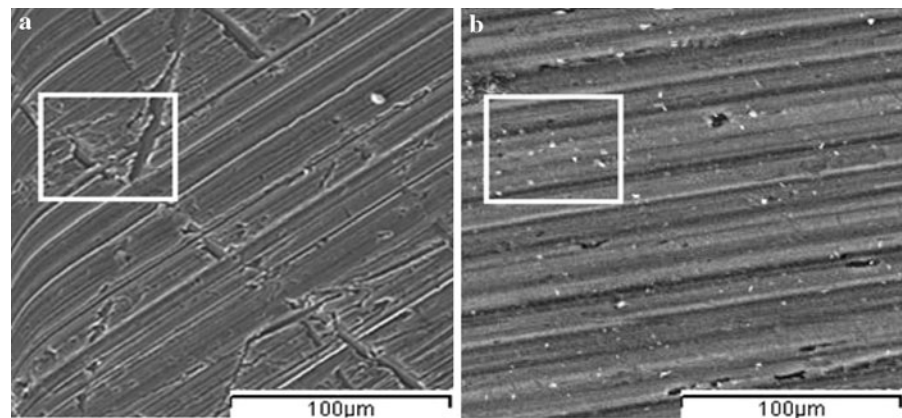


Fig. 15 The forming mechanism of self-laminating film on friction pair

Conclusion

In this article, the enhanced lubrication properties of lubricating oil with $\text{ZrO}_2/\text{SiO}_2$ composite nanoparticles as additives were reported. The $\text{ZrO}_2/\text{SiO}_2$ composite nanoparticles were synthesized and in situ modified with aluminum zirconium coupling agent. Such composite nanoparticles dispersed homogeneously in lubricating oil with good stability. The Zeta potential value indicated that static repellency of modified $\text{ZrO}_2/\text{SiO}_2$ becomes stronger than that of the as-prepared nanoparticles. The modified $\text{ZrO}_2/\text{SiO}_2$ nanoparticles were well dispersed in lubricating oil that was still transparent after 72 h. Therefore, the $\text{ZrO}_2/\text{SiO}_2$ composite nanoparticles changed from hydrophilic to hydrophobic after the surface modification. Lubrication properties of such nano-oil were investigated with four-ball friction and wear experiments. It was found that the optimized concentration of the modified $\text{ZrO}_2/\text{SiO}_2$ composite nanoparticles was 0.1 wt% and the averaged reduction of friction

coefficient was 16.24%. In this case, the wear scar diameter of the vertical was reduced by 14.59%. Moreover, the negative wear and tear was observed in thrust ring friction and wear tests when the concentration was 0.1 wt% due to the dynamic self-healing deposition effect of the nanoparticles. It was expected that the frictional heat was reduced and viscosity was increased. Therefore, the oil film was preserved at high load and the lubricating properties were enhanced.

Acknowledgments The authors acknowledge the financial support from National Science Foundation of China (50572034). B. Cai is an Oversea Taishan Scholar and thank the financial support from UJN for a new faculty.

References

- Chin-as-Castillo F, Spikes HA (2003) Mechanism of action of colloidal solid dispersions. *J Tribol* 125:552–557
- Dong JX, Hu ZS, Chen GX (1998) Controllable high-speed journal bearings lubricated with electro-rheological fluids. *Tribol Int* 31(5):219–222
- Guo QB, Rong MZ, Jia GL, Lau KT, Zhang MQ (2009) Sliding wear performance of nano- SiO_2 /short carbon fiber/epoxy hybrid composites. *Wear* 266:658–665
- Hu Z, Dong JX (1998) Study on antiwear and reducing friction additive of nanometer titanium borate. *Wear* 216:87–90
- Hu ZS, Dong JX, Chen GX (1998) Study on antiwear and reducing friction additive of nanometer ferric oxide. *Tribol Int* 31(7):355–360
- Hu ZS, Lai R, Lou F, Wang LG, Chen ZL, Chen GX, Dong JX (2002) Preparation and tribological properties of nanometer magnesium borate as lubricating oil additive. *Wear* 252:370–374
- Huang HD, Tu JP, Gan LP (2006) An investigation on tribological properties of graphite nanosheets as oil additive. *Wear* 261:140–144

- Jee Ah-Y, Lee M (2009) Surface functionalization and physicochemical characterization of diamond nanoparticles. *Curr Appl Phys* 9:e144–e147
- Kato H, Komai K (2007) Tribofilm and mail wear by tribosintering of nanometer-sized oxide particle on rubbing steel surface. *Wear* 262(2):36–41
- Lee K, Hwang Y, Cheong S, Kwon L, Kim S, Lee J (2009) Performance evaluation of nano-lubricants of fullerene nanoparticles in refrigeration mineral oil. *Curr Appl Phys* 9:e128–e131
- Liu G, Li X, Qin B, Xing D, Guo Y, Fan R (2004) Investigation of the mending effect and mechanism of copper nanoparticles on a tribologically stressed surface. *Tribol Lett* 17(4):961–966
- Merschdorf M (2002) Photoemission from multiply excited surface plasmons in Ag nanoparticles. *Appl Phys A* 20(4):547–552
- Murakami T, Ouyang JH, Sasaki S, Umeda K, Yoneyama Y (2007) High-temperature tribological properties of spark-plasma-sintered Al_2O_3 composites containing barite-type structure sulfates. *Tribol Int* 40:246–253
- Rapoport L, Leshchinsky V, Lapsker I, Volovik Y, Nepomnyashchy O, Lvovsky M (2003) Tribological properties of WS_2 nanoparticles under mixed lubrication. *Wear* 255:785–793
- Red'kin VE (2004) Lubricants with ultra-disperse diamond-graphite powder. *Chem Tech Fuels Oil* 40(3):164–170
- Song HJ, Zhang ZZ (2006) Investigation of the tribological properties of polyfluoro wax/polyurethane composite coating filled with nano-SiC or nano- ZrO_2 . *Mater Sci Eng A* 426:59–65
- Song HJ, Zhang ZZ (2008) Study on the tribological behaviors of the phenolic composite coating filled with modified nano- TiO_2 . *Tribol Int* 41:396–403
- Sui G, Zhong WH, Ren X, Wang XQ, Yang XP (2009) Structure, mechanical properties and friction behavior of UHMWPE/HDPE/carbon nanofibers. *Mater Chem Phys* 115:404–412
- Sun R, Li MJ, Gao YJ (2002) Study on the cutting properties of water-based emulsified liquid containing OA/ TiO_2 nanoparticles and tea saponins. *Tribology* 22:4–8
- Wu YY, Tsui WC, Liu TC (2007) Experimental analysis of tribological properties of lubricating oils with nanoparticle additives. *Wear* 262:819–825
- Xu T, Zhao TZ, Xu K (1997) Study on the tribological properties of ultra-dispersed diamond containing soot as an oil additive. *Tribol Int* 40(3):178–189
- Zhang M, Wang XB, Fu XS, Xia YQ (2009) Performance and anti-wear mechanism of CaCO_3 nanoparticles as a green additive in poly-alpha-olefin. *Tribol Int* 42:1029–1039
- Zhou XD, Fu X, Shi HQ, Hu ZS (2007) Lubricating properties of Cyanex 302-modified MoS_2 microspheres in base oil 500SN. *Lubr Sci* 19:71–79